

# Non-natural 3-Arylmorpholino- $\beta$ -amino Acid as a PPII Helix Inducer

Francesco Vaghi,<sup>†</sup> Raffaella Bucci,<sup>†</sup> Francesca Clerici, Alessandro Contini,<sup>\*</sup> and M. Luisa Gelmi<sup>\*</sup>

Cite This: *Org. Lett.* 2020, 22, 6197–6202

Read Online

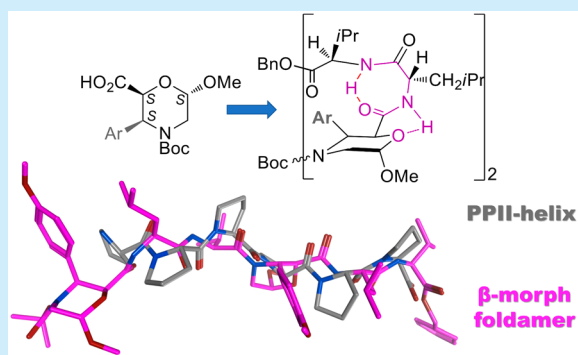
ACCESS |

Metrics & More

Article Recommendations

Supporting Information

**ABSTRACT:** A new non-natural  $\beta$ -amino acid, named 3-Ar- $\beta$ -Morph, was designed and synthesized via a regio- and diastereoselective Pd-catalyzed C(sp<sup>3</sup>)H-arylation of the corresponding 2*S*,6*S*-(6-methoxymorpholin-2-yl)carboxylic acid, readily available from glucose. According to the computational prevision and confirmed by IR and NMR data, the insertion of 3-Ar- $\beta$ -Morph in a model foldamer represents a way to stabilize a PPII-like helix through the presence of two  $\gamma$ -turns, secondary structure motifs induced by the morpholine ring, and the *trans*-tertiary amide bond.



Peptides are bioactive molecules designed by Nature to absorb numerous functions in several biological processes. Their ability to assume specific conformations and to organize in three-dimensional folded structures is driven by the encoded amino acid sequences.<sup>1,2</sup> Among the ubiquitous secondary structures in folded proteins ( $\alpha$ -helices, 3,10-helices, and  $\beta$ -sheet), the less abundant but still frequently occurring regular structure is the polyproline II helix (PPII).<sup>3</sup> This helix is characterized by  $\phi$  and  $\psi$  torsional angles of about  $-75^\circ$  and  $150^\circ$ , respectively, and, contrary to PPI, is left-handed with *trans* peptide bonds.<sup>4</sup> Its importance in biological systems emerged in recent years: from the transcription to the cell motility and from the bacterial and viral pathogenesis to amyloidogenic proteins.<sup>5</sup> Moreover, it is also at the basis of the collagen triple helix, formed by three PPIIs that coil into each other thanks to intermolecular hydrogen bonds.<sup>6</sup> PPII is also important in unfolded proteins, being considered as a transition structure between a helix and a random coil.<sup>3,7</sup> With these premises, it is clear how the synthesis of PPII structure-mimics is of relevance. Some examples of inhibitors/modulators of proline-rich-mediated protein–protein interactions are present,<sup>8–10</sup> as well as some synthetic collagen model peptides containing modified prolines.<sup>11–14</sup>

Small molecules or noncoded amino acids (AAs)<sup>15</sup> are commonly useful as inducers of a particular secondary structure. The derived peptidomimetics<sup>16–18</sup> are characterized by similar features of the target peptide<sup>19</sup> but with increased proteolytic stability.<sup>20–22</sup>

Despite the large number of protocols involving  $\beta$ -AAs for locking peptides into helices and  $\beta$ -strand conformations, their use for generating mimics of PPII structures is absent in the literature.<sup>23</sup>

Recently, we reported on the synthesis of a morpholino  $\beta$ -AA, named  $\beta$ -Morph **1**, that was inserted in peptide sequences ( $n = 1, 2$ ; R = H; Figure 1).<sup>24</sup>

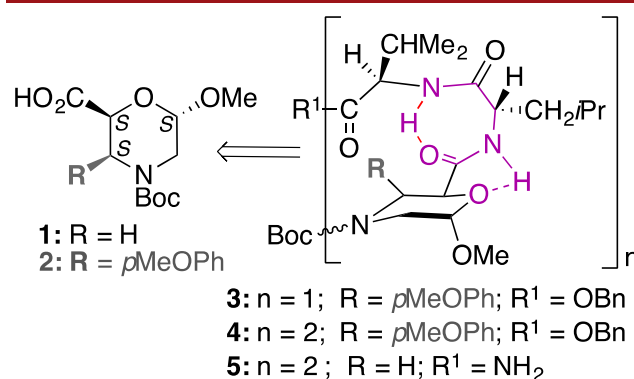


Figure 1.  $\beta$ -Morpholino-containing peptides.

Due to the formation of a strong H-bond between the oxygen of the morpholino ring and NH of amino acid  $i+1$ ,  $\gamma$ -turn/s stabilized by a H-bond between C=O and NH at positions  $i$  and  $i+2$  can be formed. Interestingly, the hexapeptide **5** (Figure 1) also showed an equilibrium between  $\alpha$ - and PPII-helices. The shift between the two geometries, facilitated by the  $\gamma$ -turn, was

Received: July 14, 2020

Published: July 30, 2020



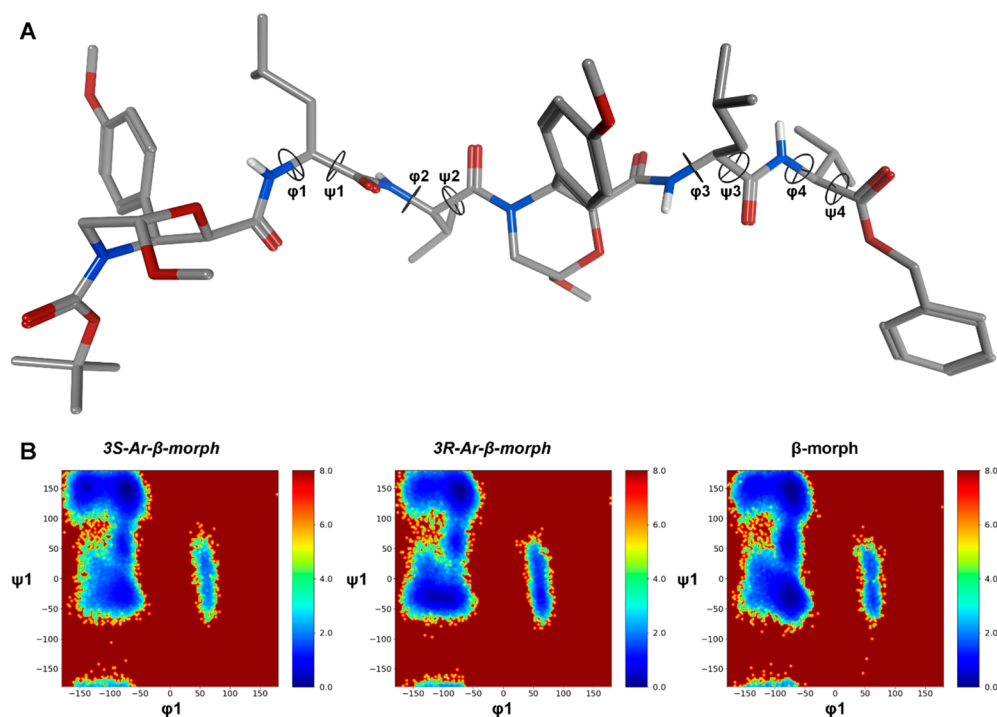


**Figure 2.** (A) Representative geometry of the most populated cluster *c0* for (3*S*)-4. (B) Heatmaps describing the relative free energy (kcal/mol) associated with different values for the  $\phi_1/\psi_1$  dihedral pair for peptides (3*S*)-4, (3*R*)-4, and 5,<sup>24</sup> containing 3*S*-Ar- $\beta$ -Morph, 3*R*-Ar- $\beta$ -Morph, and  $\beta$ -Morph, respectively. The geometrical analysis was conducted on the 1000–1500 ns section of the unbiased H-REMD replica. Heatmaps for all the considered dihedral pairs are reported in Figure S1.

attributed to the rotation of the tertiary amide bond.<sup>24</sup> In order to block this rotation, we evaluated the possibility of introducing a bulky group in the  $\alpha$ -position of the tertiary amide bond on the morpholino ring, thus stabilizing one of the two conformations.

Aiming to obtain a PPII structure, a preliminary computational study was performed evaluating the use of a 3-aryl-substituted analogue of **1** in both configurations. On the basis of computational predictions, the (2*S*,3*S*,6*S*)-6-methoxy-3-(4-methoxyphenyl)morpholine-2-carboxylic acid scaffold, named 3-Ar- $\beta$ -Morph **2** (Figure 1), was prepared by a Pd-catalyzed regio- and diastereoselective C(sp<sup>3</sup>)H-arylation. Its insertion in the same sequence reported in Figure 1 ( $n = 2$ , R = *p*MeOPh) gave a PPII-like conformation, as confirmed by IR/NMR studies, proving that 3-Ar- $\beta$ -Morph is the first non-natural  $\beta$ -AA that can be used to stabilize PPII in peptides.

## COMPUTATIONAL STUDY

As reported,<sup>24</sup> H-REMD simulations described the preferred conformations of tri- and hexapeptides containing  $\beta$ -Morph **1** successfully. Thus, we performed a prospective computational study to evaluate the role of the *p*-methoxyphenyl group at C-3 and of the stereochemical configuration at the same carbon in ruling the conformational preferences of *N*-Boc-[(*S/R*)-Ar- $\beta$ -Morph-Leu-Val]<sub>2</sub>-OBn peptide, here referred to as (3*S*)- and (3*R*)-4. H-REMD simulations were performed in explicit MeCN solvent (12 replica of 1.5  $\mu$ s each, for a total of 18  $\mu$ s of simulations). The unbiased replica was then analyzed by clustering analysis to obtain a description of the different conformations, and relative weights, accessible by the two peptides. Additionally, the backbone  $\phi$  and  $\psi$  dihedrals were analyzed on the same trajectory. Heatmaps representing the probability of occurrence of  $\phi/\psi$  dihedral pairs for each residue were produced to evidence any difference between (3*S*)- and

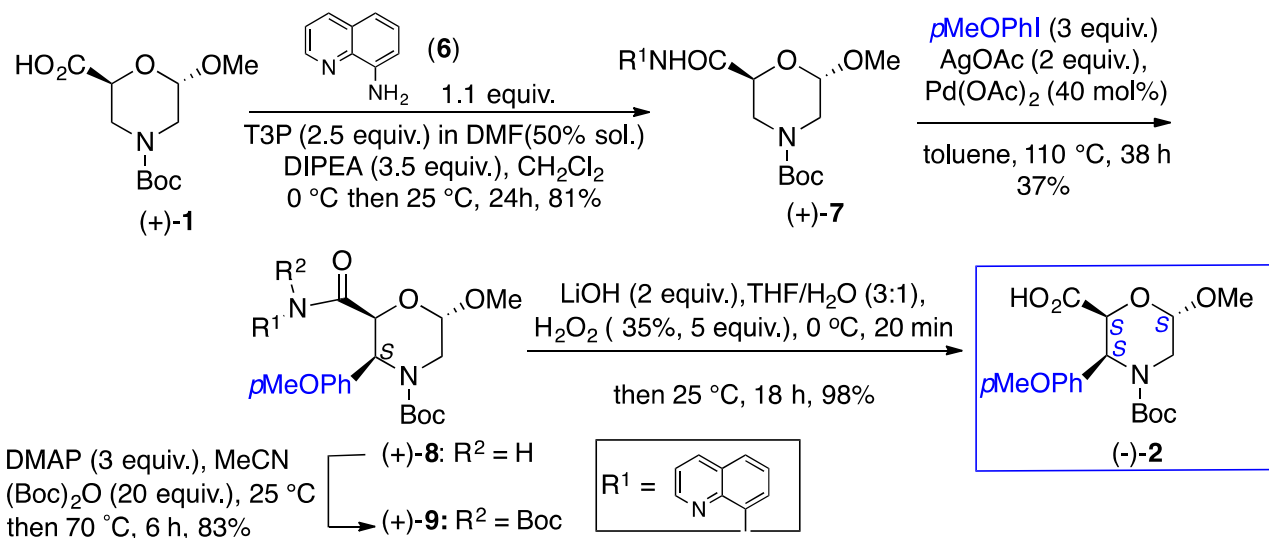
(3*R*)-4, in comparison with the peptide **5** containing **1** (Figure 1).<sup>24</sup> Results are reported in Tables 1 and S1 and in Figures 2, S1, and S2. As expected, the insertion of the aryl group at C-3 induced a significant change in the conformational preferences of peptides (3*S*)-4 and (3*R*)-4 (Figures 2 and S1), compared to **5**.

**Table 1. Representative Results for the Geometrical<sup>a</sup> and Cluster Analyses of the H-REMD Trajectory for the Unbiased Replica**

	(3 <i>S</i> )-4	(3 <i>R</i> )-4
$\phi_1$	$-54.8 \pm 43.4$	$-111.0 \pm 17.0$
$\psi_1$	$135.8 \pm 28.0$	$-33.0 \pm 9.7$
$\phi_2$	$-75.8 \pm 27.7$	$-128.5 \pm 8.9$
$\psi_2$	$152.4 \pm 21.1$	$82.7 \pm 11.1$
$\phi_3$	$-86.9 \pm 25.6$	$-72.0 \pm 11.0$
$\psi_3$	$147.0 \pm 49.4$	$-6.9 \pm 18.2$
$\phi_4$	$-75.4 \pm 26.5$	$-80.8 \pm 18.6$
$\psi_4$	$127.9 \pm 29.1$	$122.8 \pm 12.1$
<i>c0</i> pop (%) <sup>b</sup>	67.3	29.2

<sup>a</sup>Dihedral values taken from the most representative conformation of the main cluster *c0* (intervals are the mean deviations of the whole *c0* population from the centroid). <sup>b</sup>Population is reported for *c0* only (see Table TS1 for all cluster populations).

However, a different behavior was observed depending on the stereochemistry at C-3. The population of the main conformational cluster is different for (3*S*)-4 and (3*R*)-4 (67.3% and 29.2%, respectively; Tables 1 and TS1) suggesting that the former is conformationally more stable. Moreover, for (3*S*)-4, the average  $\phi$  and  $\psi$  dihedrals of the main cluster (*c0*) population are within the typical PPII-helices range (about  $-75^\circ$

Scheme 1. Synthesis of 3-Ar- $\beta$ -Morph (-)-2

and  $150^\circ$ , respectively; Table 1 and Figure 2A). Conversely, a disordered conformation is predicted for (3R)-4, where the average  $\varphi$  and  $\psi$  dihedrals of c0 do not match any well-defined secondary structure (Table 1 and Figure S2). The different behavior of (3S)-4, (3R)-4, and 5 is also well described by the heatmaps (Figures 2B and S1) obtained from the analysis of the last 500 ns of the H-REMD trajectory, representing the conformational free energy surfaces derived from the Boltzmann distributions of selected dihedral pairs. Indeed, a deep well at about  $\varphi_1 = -80^\circ$  and  $\psi_1 = 150^\circ$  can be observed for (3S)-4. Conversely, for (3R)-4, an additional and rather wide low energy region is observed at about  $\varphi_1 = -100^\circ$  and  $\psi_1 = -50^\circ$ . Furthermore, the region corresponding to the left-handed helix ( $30^\circ \leq \varphi \leq 130^\circ$  and  $-50^\circ \leq \psi \leq 100^\circ$ )<sup>25</sup> also is energetically more accessible, compared to (3S)-4. In conclusion,  $\beta$ -Morph 1 seems to favor both PP- and  $\alpha$ -helix geometries, as well as the transition region between them represented by the inverse  $\gamma$ -turn region ( $\varphi \approx -80^\circ$  and  $\psi \approx 70^\circ$ ). Conversely, (3R)-Ar- $\beta$ -Morph still induces  $\alpha$ - and PP-helices, but with a less favored inverse  $\gamma$ -turn region. Moreover, the left-handed  $\alpha$ -helix appears to be more accessible with respect to foldamers containing 1 or 2. Interestingly, this latter seems to be able to stabilize the PP-region mainly. We also investigated if 4 might replace polyproline in a biological complex. Using the structure of the proflin-poly-L-proline complex<sup>26</sup> as a reference, we performed MD simulations and binding energy calculations<sup>27</sup> on both the reference and the model where (3S)-4 replaced the polyproline chain. This latter remained stable during 100 ns of simulation and computed binding energy resulted lower than that of the reference (Figure S3 and Table TS2).

## ■ SYNTHESIS OF THE NEW SCAFFOLD 2

The enantiopure  $\beta$ -Morph (+)-1 (Figure 1, R = H) was prepared starting from glucose.<sup>24</sup> First, 1 was transformed into amide 7 by reaction with 8-aminoquinoline (6). As reported,<sup>28</sup> a regio- and diastereoselective Pd-catalyzed C(sp<sup>3</sup>)H-arylation could be mediated by the Pd-coordinating nitrogen of quinoline ring. Amide 7 (43%) was first prepared by using a reported protocol.<sup>28</sup> On the other hand, a strong improvement in the yield was achieved by activation of 1 with propylphosphonic anhydride [T3P, 2.5 equiv; 50% DMF solution in CH<sub>2</sub>Cl<sub>2</sub>, DMAP (3.5 equiv), 0 °C, 1 h; then 24 h at 25 °C] followed by

reaction with 6 (1.1 equiv, 25 °C, 24 h) giving (+)-7 in 81% yield (Scheme 1).

The arylation at C-3 for a similar compound of 7 (10% yield) is reported [Pd(OAc)<sub>2</sub> (0.1 equiv), AcOAg (2 equiv), MeOPhI (3 equiv) toluene, reflux, 38 h)].<sup>28</sup> The same protocol, starting from 7 and *p*-iodoanisole, gave analogous yields of 8. Several attempts were performed to optimize this procedure. While the use of toluene was found to be crucial (other solvents inhibit the reaction), incrementing the amount of Pd(OAc)<sub>2</sub>—from 0.2 to 0.4 equiv—increased the yield up to 37% (63% recovery starting material). Unfortunately, no improvement was observed by changing the catalyst (Cu(OAc)<sub>2</sub>, Cu(TFA)<sub>2</sub>, Pd(TFA)<sub>2</sub>, PdCl<sub>2</sub>) or the oxidant (AgTFA instead of AcOAg). The reaction is regio- and diastereoselective, affording only compound (+)-8 having the aryl moiety in *cis* relationship with the carbonyl group.

To synthesize the deprotected carboxylic acid 2, *N*-Boc amide (+)-9 was prepared first [(Boc)<sub>2</sub>O (20 equiv), DMAP (3 equiv), MeCN, 70 °C, 6 h; 83%]. Its hydrolysis [LiOH·H<sub>2</sub>O (2 equiv)/H<sub>2</sub>O<sub>2</sub> (35%, 5 equiv), THF/H<sub>2</sub>O (3:1), 25 °C, 18 h] gave (-)-2 (98%).

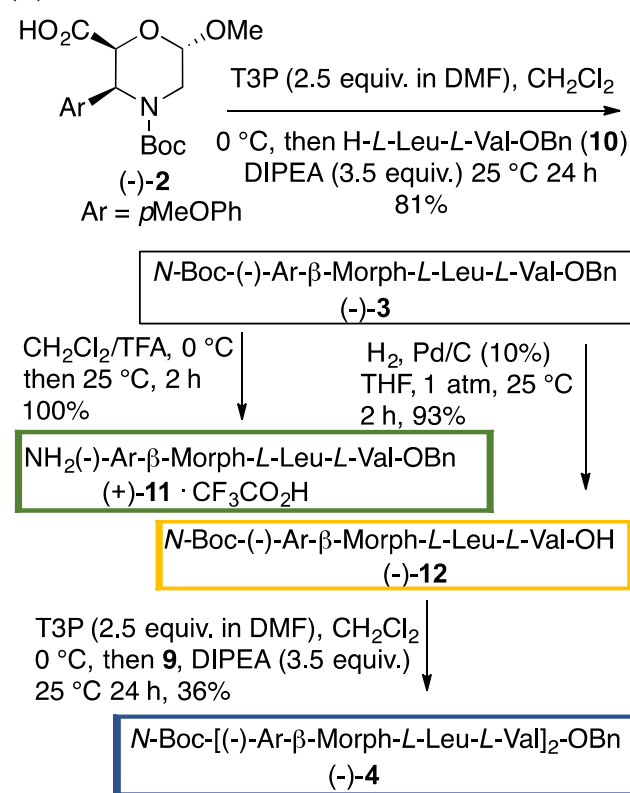
## ■ FOLDAMER SYNTHESIS

Foldamer syntheses (Scheme 2) were optimized by using different coupling agents. Starting from (-)-2 and dipeptide 10, T3P [(DMF/DMAP solution) in CH<sub>2</sub>Cl<sub>2</sub> (0 °C, 1 h then 24 h at 25 °C)] is the most efficient coupling agent, giving tripeptide (-)-3 in 81% yield. Tripeptide was selectively deprotected (TFA, CH<sub>2</sub>Cl<sub>2</sub>, 25 °C, 2 h), giving (+)-11 (quantitative yield). A reductive debenzoylation of 3 (H<sub>2</sub>, Pd/C, THF, 1 atm., 25 °C, 2 h) provided (-)-12 (93%). The coupling of 11 with 12 gave low yield of hexapeptide 4 (17 and 8%, respectively) when using HOBt/EDC or HOBt [(1.1 equiv)/EtCN-oxime (1.1 equiv)/DIPEA (2.1 equiv)]. T3P was the best coupling agent, improving the yield of (-)-4 (36%). The steric demanding coupling reaction probably affected the high reaction yields.

## ■ IR CHARACTERIZATION

FTIR analysis was performed on a solid sample of (-)-4 (Figure S8). The PP-conformation is confirmed by the presence of a peak around 1640 cm<sup>-1</sup>, corresponding to the PP-characteristic C=O stretching frequency (amide I).<sup>29</sup>

Scheme 2. Synthesis of Tripeptide (–)-3 and Hexapeptide (–)-4



### NMR CHARACTERIZATION

The stereochemistry of (–)-2 at C-3 was assigned based on  $J$  values and NOESY experiments. The *trans* disposition of H-2/H-3 is excluded by the  $J$  value (5.1 Hz), and a distorted morpholino chair is suggested ( $J_{5_{ax},6} = 8.9\text{ Hz}$ ,  $J_{5_{eq},6} = 5.4\text{ Hz}$ ). NOEs were detected between H-2/Boc (w) and aryl group with H-2, H-3, and H-5<sub>ax</sub> indicating the pseudoaxial disposition of the aryl moiety *cis* with respect to the carboxylic function (Figures S4, Table TS3).

Tripeptides (–)-3 and hexapeptide (–)-4 were characterized by NMR ( $^1\text{H}$ ,  $^{13}\text{C}$ , COSY, TOCSY, HMBC, HMQC, NOESY; 600 MHz) in  $\text{CD}_3\text{CN}$  solution, and  $\delta$  values of morpholino and  $\alpha$ -AA protons were unequivocally assigned (Tables S4 and S5). Tripeptide 3 showed several similarities<sup>24</sup> with the tripeptide of Figure 1 ( $n = 1$ , R = H, R<sup>1</sup> = Bn): a  $\gamma$ -turn is present at C-terminus. As reported in Figure S5, weak NOEs are those between  $\text{NH}_{\text{Leu}}$  with  $\text{OMe}_{\text{Morph}}$ , H-6, and H-2, indicating its orientation toward the oxygen region of the ring. The formation of the  $\gamma$ -turn is supported by the spatial proximity of  $\text{NH}_{\text{Val}}$  with the leucine moiety. Furthermore, low  $\delta\Delta/\Delta T$  values (273–323 K; Figure S6) for  $\text{NH}_{\text{Val}}$  (–1.8 ppb  $\text{K}^{-1}$ ) and  $\text{NH}_{\text{Leu}}$  (–2.2 ppb  $\text{K}^{-1}$ ) were detected. Accordingly, a H-bond between  $\text{NH}_{\text{Val}}$  and  $\text{C}=\text{O}_{\text{Morph}}$  is suggested, driven by a second strong H-bond between  $\text{NH}_{\text{Leu}}$  and the oxygen of the ring.

Interestingly, the NMR analysis of (–)-4 showed the presence of a main conformer (80:20,  $^1\text{H}$  NMR data). Very low  $\delta\Delta/\Delta T$  values (273–333 K) for all NHs ranging from –2.8 to –2 ppb  $\text{K}^{-1}$  (Figure 3C) were found for the main isomer, supporting a strong H-bond network, as indicated for 3. NOEs of compound (–)-4 are shown in Figures 3A and S7. Similar spatial proximities between  $\text{NH}_{\text{Leu}2}$  and  $\text{NH}_{\text{Leu}5}$  with the acetal region of the corresponding morpholine ring at positions 1 and 4

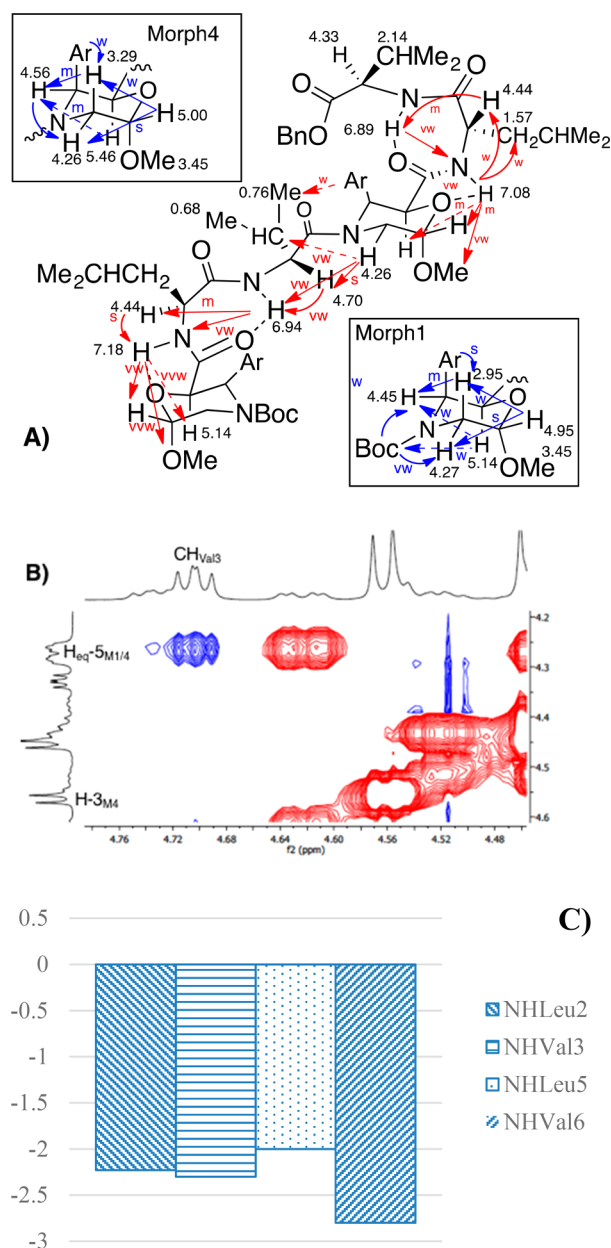


**Figure 3.** NMR data for hexapeptide (–)-4 ( $\text{CD}_3\text{CN}$ , mM, 600 MHz): (A) NOEs of morpholino ring protons (blue arrows) and between the different AAs (red arrows) and H-bonds (dotted lines). (B) Zoom of Val<sub>3</sub>/Morph<sub>4</sub> region. (C)  $\delta\Delta/\Delta T$  NH values (273–333 K).

are present, supporting the formation of two  $\gamma$ -turns. Spatial proximities between  $\text{CH}_{\text{Val}3}$  and protons of morpholine-4 are diagnostic for the prediction of the main conformer. NOEs were detected between  $\text{CH}_{\text{Val}3}$  and  $\text{H}_{\text{eq-}5\text{M}1/4}$  but not with H-3<sub>Morph4</sub> (Figure 3B), thus indicating the orientation of  $\text{C}=\text{O}$  toward the aryl region. As a result, the *E*-conformer is suggested for the tertiary amide bond.

In conclusion, starting from our previous knowledge indicating that scaffold 1 is able to generate a mixture of  $\alpha$ - and PPII-like helices, we designed the new scaffold (–)-2. We demonstrated by computational, IR and NMR data that 2 represents the first  $\beta$ -AA able to induce a PPII helix when inserted in a model foldamer due to the presence of a hindered aryl-substituent at C-3 that blocks the rotation of the tertiary amide bond favoring the *trans*-conformation.

## ■ ASSOCIATED CONTENT

## ■ Supporting Information

The Supporting Information is available free of charge at <https://pubs.acs.org/doi/10.1021/acs.orglett.0c02331>.

Computational details, synthetic protocols, and IR, <sup>1</sup>H NMR, <sup>13</sup>C NMR spectra for compounds 2–4, 7–9, 11, and 12 (PDF)

## ■ AUTHOR INFORMATION

## Corresponding Authors

**Alessandro Contini** – DISFARM-Sez. Chimica Generale e Organica “A. Marchesini”, Università degli Studi di Milano, 20133 Milano, Italy; [orcid.org/0000-0002-4394-8956](https://orcid.org/0000-0002-4394-8956);  
Email: [alessandro.contini@unimi.it](mailto:alessandro.contini@unimi.it)

**M. Luisa Gelmi** – DISFARM-Sez. Chimica Generale e Organica “A. Marchesini”, Università degli Studi di Milano, 20133 Milano, Italy; [orcid.org/0000-0003-0743-5499](https://orcid.org/0000-0003-0743-5499);  
Email: [marialuisa.gelmi@unimi.it](mailto:marialuisa.gelmi@unimi.it)

## Authors

**Francesco Vaghi** – DISFARM-Sez. Chimica Generale e Organica “A. Marchesini”, Università degli Studi di Milano, 20133 Milano, Italy

**Raffaella Bucci** – DISFARM-Sez. Chimica Generale e Organica “A. Marchesini”, Università degli Studi di Milano, 20133 Milano, Italy

**Francesca Clerici** – DISFARM-Sez. Chimica Generale e Organica “A. Marchesini”, Università degli Studi di Milano, 20133 Milano, Italy; [orcid.org/0000-0003-3483-5914](https://orcid.org/0000-0003-3483-5914)

Complete contact information is available at:

<https://pubs.acs.org/doi/10.1021/acs.orglett.0c02331>

## Author Contributions

†F.V. and R.B. contributed equally.

## Notes

The authors declare no competing financial interest.

## ■ REFERENCES

- (1) Donate, L. E.; Rufino, S. D.; Canard, L. H. J.; Blundell, T. L. Conformational Analysis and Clustering of Short and Medium Size Loops Connecting Regular Secondary Structures: A Database for Modeling and Prediction. *Protein Sci.* **1996**, *5* (12), 2600–2616.
- (2) Hruby, V. J.; Li, G.; Haskell-Luevano, C.; Shenderovich, M. Design of Peptides, Proteins, and Peptidomimetics in Chi Space. *Biopolymers* **1997**, *43* (3), 219–266.
- (3) Adzhubei, A. A.; Sternberg, M. J. E.; Makarov, A. A. Polyproline-II Helix in Proteins: Structure and Function. *J. Mol. Biol.* **2013**, *425* (12), 2100–2132.
- (4) Wilhelm, P.; Lewandowski, B.; Trapp, N.; Wennemers, H. A Crystal Structure of an Oligoproline PPII-Helix, at Last. *J. Am. Chem. Soc.* **2014**, *136* (45), 15829–15832.
- (5) Moradi, M.; Babin, V.; Sagui, C.; Roland, C. A Statistical Analysis of the PPII Propensity of Amino Acid Guests in Proline-Rich Peptides. *Biophys. J.* **2011**, *100* (4), 1083–1093.
- (6) Traub, W.; Piez, K. A. *The Chemistry and Structure of Collagen*; Anfinsen, C. B., Edsall, J. T., Richards, F. M. B. T.-A., Eds.; Academic Press, 1971; Vol. 25, pp 243–352.
- (7) Hiltner, W. A.; Hopfinger, A. J.; Walton, A. G. Helix-Coil Controversy for Polyamino Acids. *J. Am. Chem. Soc.* **1972**, *94*, 4324–4327.
- (8) Reuter, C.; Opitz, R.; Soicke, A.; Dohmen, S.; Barone, M.; Chiha, S.; Klein, M. T.; Neudörfel, J.-M.; Kühne, R.; Schmalz, H.-G. Design and Stereoselective Synthesis of ProM-2: A Spirocyclic Diproline Mimetic

with Polyproline Type II (PPII) Helix Conformation. *Chem. - Eur. J.* **2015**, *21* (23), 8464–8470.

(9) Raghavan, B.; Skoblenick, K. J.; Bhagwanth, S.; Argintaru, N.; Mishra, R. K.; Johnson, R. L. Allosteric Modulation of the Dopamine D2 Receptor by Pro-Leu-Gly-NH2 Peptidomimetics Constrained in Either a Polyproline II Helix or a Type II  $\beta$ -Turn Conformation. *J. Med. Chem.* **2009**, *52* (7), 2043–2051.

(10) Zaminer, J.; Brockmann, C.; Huy, P.; Opitz, R.; Reuter, C.; Beyersmann, M.; Freund, C.; Müller, M.; Oschkinat, H.; Kühne, R.; et al. Addressing Protein–Protein Interactions with Small Molecules: A Pro-Pro Dipeptide Mimic with a PPII Helix Conformation as a Module for the Synthesis of PRD-Binding Ligands. *Angew. Chem., Int. Ed.* **2010**, *49* (39), 7111–7115.

(11) Lee, S.-G.; Lee, J. Y.; Chmielewski, J. Investigation of PH-Dependent Collagen Triple-Helix Formation. *Angew. Chem.* **2008**, *120* (44), 8557–8560.

(12) Hentzen, N. B.; Islami, V.; Köhler, M.; Zenobi, R.; Wennemers, H. A Lateral Salt Bridge for the Specific Assembly of an ABC-Type Collagen Heterotrimer. *J. Am. Chem. Soc.* **2020**, *142* (5), 2208–2212.

(13) Detert, H.; Rose, B.; Mayer, W.; Meier, H. Herstellung von 1,5-Cyclooctadiin Und 1,3,5,7-Cyclooctatetraen Aus 1,5-Cyclooctadien. *Chem. Ber.* **1994**, *127* (8), 1529–1532.

(14) Maaßen, A.; Gebauer, J. M.; Theres Abraham, E.; Grimm, I.; Neudörfel, J.-M.; Kühne, R.; Neudorf, L.; Baumann, U.; Schmalz, H.-G. Triple-Helix-Stabilizing Effects in Collagen Model Peptides Containing PPII-Helix-Preorganized Diproline Modules. *Angew. Chem., Int. Ed.* **2020**, *59* (14), 5747–5755.

(15) Bonetti, A.; Clerici, F.; Foschi, F.; Nava, D.; Pellegrino, S.; Penso, M.; Soave, R.; Gelmi, M. L. Syn/Anti Switching by Specific Heteroatom – Titanium Coordination in the Mannich-Like Synthesis of 2, 3-Diaryl- $\beta$ -Amino Acid Derivatives. *Eur. J. Org. Chem.* **2014**, *2014*, 3203–3209.

(16) Bucci, R.; Contini, A.; Clerici, F.; Beccalli, E. M.; Formaggio, F.; Maffucci, I.; Pellegrino, S.; Gelmi, M. L. Fluoro-Aryl Substituted  $\alpha$ , $\beta$ , $\gamma$ -Peptides in the Development of Foldameric Antiparallel  $\beta$ -Sheets: A Conformational Study. *Front. Chem.* **2019**, *7*, 192.

(17) Bucci, R.; Giofrè, S.; Clerici, F.; Contini, A.; Pinto, A.; Erba, E.; Soave, R.; Pellegrino, S.; Gelmi, M. L. Tetrahydro-4 H-(Pyrrolo[3,4-d]isoxazol-3-yl)methanamine: A Bicyclic Diamino Scaffold Stabilizing Parallel Turn Conformations. *J. Org. Chem.* **2018**, *83* (19), 11493–11501.

(18) Bucci, R.; Bonetti, A.; Clerici, F.; Contini, A.; Nava, D.; Pellegrino, S.; Tessaro, D.; Gelmi, M. L. Tandem Tetrahydroisoquinoline-4-Carboxylic Acid/ $\beta$ -Alanine as a New Construct Able To Induce a Flexible Turn. *Chem. - Eur. J.* **2017**, *23* (45), 10822–10831.

(19) Contini, A.; Ferri, N.; Bucci, R.; Lupo, M. G.; Erba, E.; Gelmi, M. L.; Pellegrino, S. Peptide Modulators of Rac1/Tiam1 Protein-Protein Interaction: An Alternative Approach for Cardiovascular Diseases. *Pept. Sci.* **2018**, *110* (5), No. e23089.

(20) Pellegrino, S.; Tonali, N.; Erba, E.; Kaffy, J.; Taverna, M.; Contini, A.; Taylor, M.; Allsop, D.; Gelmi, M. L.; Ongeri, S.  $\beta$ -Hairpin Mimics Containing a Piperidine-Pyrrolidine Scaffold Modulate the  $\beta$ -Amyloid Aggregation Process Preserving the Monomer Species. *Chem. Sci.* **2017**, *8* (2), 1295–1302.

(21) Bucci, R.; Das, P.; Iannuzzi, F.; Feligioni, M.; Gandolfi, R.; Gelmi, M. L.; Reches, M.; Pellegrino, S. Self-Assembly of an Amphipathic  $\alpha\alpha\beta$ -Tripeptide into Cationic Spherical Particles for Intracellular Delivery. *Org. Biomol. Chem.* **2017**, *15*, 6773–6779.

(22) Heck, T.; Limbach, M.; Geueke, B.; Zacharias, M.; Gardiner, J.; Kohler, H.-P.; Seebach, D. Enzymatic Degradation of  $\beta$ - and Mixed  $\alpha,\beta$ -Oligopeptides. *Chem. Biodiversity* **2006**, *3*, 1325.

(23) Craven, T. W.; Bonneau, R.; Kirshenbaum, K. PPII Helical Peptidomimetics Templated by Cation- $\pi$  Interactions. *ChemBioChem* **2016**, *17* (19), 1824–1828.

(24) Bucci, R.; Contini, A.; Clerici, F.; Pellegrino, S.; Gelmi, M. L. From Glucose to Enantiopure Morpholino  $\beta$ -Amino Acid: A New Tool for Stabilizing  $\gamma$ -Turns in Peptides. *Org. Chem. Front.* **2019**, *6* (7), 972–982.

(25) Novotny, M.; Kleywegt, G. J. A Survey of Left-Handed Helices in Protein Structures. *J. Mol. Biol.* **2005**, *347* (2), 231–241.

(26) Mahoney, N. M.; Janmey, P. A.; Almo, S. C. Structure of the Profilin-Poly-L-Proline Complex Involved in Morphogenesis and Cytoskeletal Regulation. *Nat. Struct. Mol. Biol.* **1997**, *4* (11), 953–960.

(27) Maffucci, I.; Contini, A. Improved Computation of Protein–Protein Relative Binding Energies with the Nwat-MMGBSA Method. *J. Chem. Inf. Model.* **2016**, *56* (9), 1692–1704.

(28) Shang, M.; Feu, K. S.; Vantourout, J. C.; Barton, L. M.; Osswald, H. L.; Kato, N.; Gagaring, K.; McNamara, C. W.; Chen, G.; Hu, L.; et al. Modular, Stereocontrolled C $\beta$ –H/C $\alpha$ –C Activation of Alkyl Carboxylic Acids. *Proc. Natl. Acad. Sci. U. S. A.* **2019**, *116* (18), 8721–8727.

(29) Dukor, R. K.; Keiderling, T. A. Mutarotation Studies of Poly-L-Proline Using FTIR, Electronic and Vibrational Circular Dichroism. *Biospectroscopy* **1996**, *2* (2), 83–100.